

Sigma-Delta Control of a Biased and Initially-Displaced MEMS Microphone

Andrew Steinmann* N. Eva Wu*
Quang T. Su** Ronald N. Miles**

*Electrical and Computer Engineering Department, Binghamton University, Binghamton, NY (e-mail: asteinm1@binghamton.edu, evawu@binghamton.edu)

** Mechanical Engineering Department, Binghamton University, Binghamton, NY, (e-mail: quang.su@binghamton.edu, miles@binghamton.edu)

Abstract: This paper extends an earlier work that achieved resonance damping of a micro-machined directional microphone by embedding it in a compensated sigma-delta modulator (Wu et al., 2004). The goal was to combat the quadratic nonlinearity in the electrostatic force. The new developments in this paper include the use of a different capacitive device that is also biased to allow more effective readout, and the consideration of the dependence of the electrostatic force on the displacement of the microphone diaphragm, which was ignored in the earlier work. This paper discusses signal level adjustment to correct the effect of the asymmetry due to the bias, and partial feedback linearization to mitigate the nonlinearity in the electrostatic force due to the membrane displacement. Background information is given on the microphone and the damping scheme is explained. Simulation results of the control loop using Simulink are presented, where the full nonlinear model of the electrostatic force transducer is included. In addition, preliminary results of simulated linear circuit implementation of the sigma-delta control loop Multisim are also presented. This paper also investigates the robustness of the damping scheme with respect to uncertainties in stiffness and mass in the design model.

1. INTRODUCTION

A biologically inspired directional MEMS microphone has been developed by Miles et al. (2005). The microphone is modelled after the ear drums of the fly, *Ormia ochracea*, which has the unique ability to localize sound with an accuracy of 2 degrees despite the small separation between the ear drums (Mason et al., 2001). Fig.1 shows a microphone diaphragm concept inspired by *Ormia ochracea*'s ear drums. The microphone under consideration in this paper has a diaphragm with dimensions of 2 mm x 1 mm and thickness of approximately 1 μ m. The diaphragm is designed to vibrate in response to sound pressure gradients as a rigid body which sits on a pivot enabling rotational motion. The rotational motion results from a pressure difference between each side of the diaphragm.

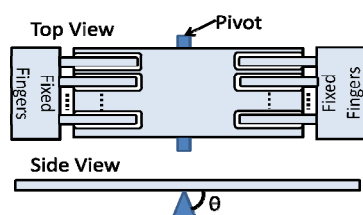


Fig.1 Comb Finger Microphone

In order to transduce the sound-induced motion of the diaphragm into an electronic signal, each side of the diaphragm has interdigitated comb fingers. These fingers may be used as a grating in an optical detection scheme. In addition, they form a variable capacitor between the sets of movable fingers and the sets of fixed fingers. The comb fingers, which create the capacitance can be seen in Fig.1. These capacitors allow for electrostatic actuation, which may be used to bias the device as well as apply a control signal. The force (or moment) applied by the electrostatic actuation is a nonlinear function of both the applied voltage across the capacitor, and the current position of the diaphragm. These two nonlinearities present challenges in the design of an active damping control scheme.

The dominant motion of the microphone diaphragm consists of pure rotation about the pivot shown in Fig.1. The motion of the system may be represented by the following governing equation

$$I\ddot{\theta} + c_t\dot{\theta} + k_t\theta = M_s + M_e, \quad (1)$$

where M_e is the moment applied to the diaphragm by the electrostatic force, M_s is the moment applied due to external sound, θ is the angular displacement, I is the mass moment of inertia, c_t is the torsional dashpot damping coefficient, and k_t is the torsional stiffness. We have shown that this equation provides an accurate model of the diaphragm's motion over most of the audible range of frequencies (Miles et al., 2009a).

One major advantage of our microphone as compared to current directional microphones is the significantly lowered noise floor. Our microphones are designed to reduce the effect from the Boltzmann thermal noise by minimizing the passive damping of the diaphragms. We have demonstrated a noise floor of 35.6 dBA compared to 47.9 dBA of current directional microphones (Miles et al., 2009a). The low noise design is made possible through the use of an optical detection method which does not require the closely spaced electrodes used with capacitive sensing that add damping (Cui et al., 2006). Minimizing the passive damping is attained at the expense of a large resonance in the system, which occurs within the range of human hearing and therefore is unacceptable for audio applications. Previous work has shown that by introducing a simple analog feedback controller, the resonance can be reduced while still maintaining the low noise floor (Miles et al., 2009b, Bicen et al., 2009). Although the analog feedback control was able to improve the closed loop performance, it was not able to meet all of the desired specifications due to the nonlinearities in the capacitive transducer of the microphone.

The primary goal of this paper is to demonstrate a possible control scheme that is able to circumvent the major nonlinearities of the capacitive actuation of the microphone and to reduce the influence of the resonance on the response. The scheme involves applying a static bias voltage along with the control voltage to one of the two capacitors in Fig.1. The basic idea presented in Wu et al. (2004) for an unbiased device will be followed with the following aspects of new development, which were proposed by Wu (2008). First, additional design steps are taken to insure that the sigma-delta control loop will maintain balanced operation around the bias point. Second, in considering the nonlinearities in the capacitive actuation, the functional dependence of the electrostatic moment on the diaphragm's displacement is dealt with; it has been treated as a constant previously. In addition, more accurate parameters are provided for the capacitive actuation and rotational modes. Furthermore, a preliminary robustness study is performed to determine the sensitivity of the digitally controlled microphone to parameter uncertainties. Robustness is a particularly important concern in this design because of the cost associated with finely tuning each controller to achieve desired performance levels for batches of micro-fabricated devices. These improvements are important steps in the design process of the control scheme.

The paper is organized as follows. Section 2 provides necessary background information by summarizing the earlier work, upon which the work reported in this paper is built, and describing the model of the device used in this study. Section 3 explains how the asymmetry introduced by the bias in the device, and the nonlinearity in the electrostatic force due to the displacement of the microphone membrane are compensated. Section 3 also presents the simulation results obtained using Simulink. Section 4 introduces a preliminary circuit implementation and Section 5 concludes the paper.

2. BACKGROUND

2.1 Summary of previous work

Wu, Miles, and Aydin (2004) introduced a control loop which uses a Sigma-Delta modulator as a way to circumvent

the nonlinearity associated with the electrostatic force of a parallel-plate capacitive microphone in an attempt to damp its resonance. Sigma-delta has been used as an oversampled ADC which converts an audio signal into a binary signal that has information stored in the density of a high frequency pulse train. Despite the equivalent digital signal being only 1-bit, it provides a resolution comparable to a 16-bit conventional ADC, depending on the amount of oversample (Aziz et al. 1996). Previous work has shown that sigma-delta was able to successfully control digital accelerometers (Kraft 1997 & Lemkin et al. 1999). The system in question in this paper and the paper published in 2004 has two problems that were not present in the digital accelerometer example.

- (1) The open-loop response of the microphone's rocking mode has a sharp resonance which must be flattened to be usable in audio applications.
- (2) The bandwidth of the microphone is two orders of magnitude wider than that of the accelerometer.

The paper by Wu et al. (2004) has demonstrated via nonlinear simulations that the large resonance (problem 1) in an unbiased microphone of parallel capacitor type can be eliminated to improve the tracking of the input sound pressure, assuming the electrostatic force depends only on the voltage across the parallel capacitor and ignoring the effects from the diaphragm's motion. In that setting, the control voltages are applied to both sides of the diaphragm to pull it in alternate intervals. A bias voltage is required, however, to benefit optical sensing for the purpose of readout and feedback. Since 2004, digital signal processors and field programmable gate arrays have improved, allowing the required sampling rate to be achieved without much difficulty. This paper expands the earlier work by including the nonlinear effect caused by the motion of the membrane around an operating point. Due to the bias voltage required to enhance the optical sensing, the microphone must operate asymmetrically around an operating point. To deal with this asymmetry, the signal levels of the bipolar output are adjusted to symmetry by inverting the nonlinearity around the bias. To circumvent the nonlinearity due to the diaphragm's motion a partial feedback linearization is introduced.

2.2 Microphone and compensator models

The microphone considered in this paper is of comb-finger type. The governing equation of the comb finger microphone is given in equation (2).

$$I\ddot{\theta} + c_t\dot{\theta} + k_t(\theta - \theta_0) = M, \quad (2)$$

where M is the moment applied to the diaphragm, θ is the angular displacement, θ_0 is the initial displacement, I is the mass moment of inertia, c_t is the torsional dashpot coefficient and k_t is the torsional stiffness. Nominal values for these parameters are identified from acoustic response measurements using a laser vibrometer (Miles et al., 2009a) and are summarized in Table 1.

The moment applied to the diaphragm, M , is composed of two parts, the moment due to external sound, M_s , and the electrostatic moment, M_e . The moment caused by external sound for a plane wave travelling along the length of the diaphragm is related to the pressure input by the following equation:

$$M_s = \frac{I_A \partial P}{c_p \partial x}, \quad (3)$$

where I_A is area moment of inertia and c_p is the speed of sound. The microphone responds to pressure gradient and has been shown to exhibit the typical figure “8” directivity pattern (Cui et al. 2006, Miles et al., 2009a). The electrostatic moment is described by,

$$M_e = f(\theta)V^2. \quad (4)$$

Description	Value	Unit
Mass moment of inertia (I)	7.45E-15	kg m ²
Torsional Dashpot (c_t)	6.45E-12	Nms/rad
Torsional Stiffness (k_t)	7.58E-07	Nm/rad
Damping ratio	0.0429	unitless
Natural frequency	10086	Rad/s
Area moment of inertia (I_a)	7.65E-13	m ⁴

Table 1 Nominal parameters and relevant constants of the microphone model

Fig. 2 shows a typical $f(\theta) = 0.5\partial C/\partial\theta$ for a capacitive microphone where the capacitance is due to interdigitated fingers as in the diaphragm of fig. 1, and indicates the initial angular displacement, θ_0 , selected operating point, θ^* , and the region identified by an experimental approximation. A least-squares fit to data by a quadratic function around the operating point is experimentally obtained by applying a quasi-static voltage and measuring the diaphragm deflection using a laser vibrometer (Su et al., 2009).

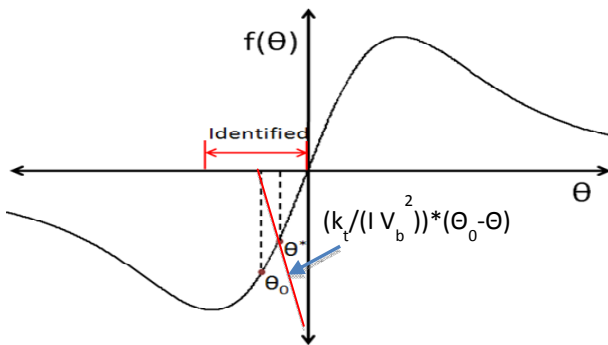


Fig.2 Approximate $f(\theta)$ which indicates original displacement, operating point and experimentally identified region

The ideal microphone has a flat frequency response over all audible frequencies. Thus the goal of the closed loop system is to mimic the ideal microphone as closely as possible, by creating a pass band from 20 Hz to 20 kHz. A compensator similar to that in Wu et al. (2004) is designed by loop-shaping to remove the resonant peak of the nominal microphone and ensure that the required bandwidth of the system is met. The transfer function in (5), represents a notch filter which perfectly cancels the resonant peak of the identified model.

$$H(s) = \frac{7.4515 \cdot 10^{-15} s^2 + 6.45 \cdot 10^{-12} s + 7.58 \cdot 10^{-7}}{s^2 + (2.513 \cdot 10^5) s}. \quad (5)$$

Although this design approach is inherently not robust due to the required knowledge of the system parameters in order to cancel the peak, the sigma-delta control loop turns out to be highly tolerant to variations in the microphone’s parameters.

A further demonstration of the robustness is described in the discussion of the simulation results.

3. SIGMA-DELTA CONTROL OF THE BIASED MICROPHONE

3.1 Gain calculation and partial feedback linearization

Fig.3 shows the Sigma-Delta control loop used to provide active damping and overcome the nonlinearities of the capacitive transducer. The external sound pressure is converted to a moment through an internal microphone operation and is added to the moment caused by the electrostatic force due to the applied voltage, as seen in (1). The combined moment is subject to the microphone dynamics and the angular deflection of the diaphragm is sensed by an optical sensor. The sensed output is applied to an analog notch filter, which is designed to cancel the resonance of the nominal microphone model. Following the filter is a sample and hold circuit and the 1-bit quantizer used to provide the digital output of the sigma-delta loop. The digital output of the quantizer encodes the input signal in the density of the pulse train. The digital output is converted back into a voltage and is passed through a signal level adjuster used to cancel the V^2 nonlinearity in the transducer. A bias voltage is added to the modified pulse train and then multiplied by a variable correction gain, which helps insure an effective linear operation.

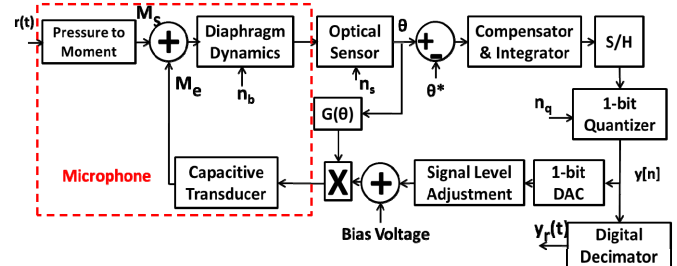


Fig.3 Sigma-Delta Control Loop (Wu, 2008)

The applied moment due to a capacitive transducer can be expressed as in equation (4), where $f(\theta)$ is a nonlinear function representing the change of capacitance with respect to the rotation, θ , and V is the voltage applied to the capacitor.

It is critical to the operation of the sigma-delta modulator that the electrostatic moment be symmetric about its nominal value. To insure that this condition is met, the appropriate signal levels must be chosen to deal with the V^2 nonlinearity and a feedback linearization gain dependent on the angular displacement, θ , must be introduced to deal with the $f(\theta)$ nonlinearity.

The signal levels are chosen so the positive signal level has the same effect as the negative signal level. To ensure that this is correct, the magnitude difference between the positive signal level and the bias voltage must equal the difference between the bias voltage level and the negative signal level. For a bias voltage, V_b , a positive signal level, V_p , a negative signal level, V_n , equation (6) must hold.

$$(V_b + V_p)^2 - V_b^2 = V_b^2 - (V_b + V_n)^2 \quad (6)$$

By fixing the positive and bias voltages, a negative voltage can be determined by solving equation (7).

$$V_n^2 - 2V_b V_n + (2V_b V_p + V_p^2) = 0 \quad (7)$$

The simulation in this paper uses a bias voltage of 3 V, a positive signal level of 1 V, and a negative signal of -1.585 V. These signal levels are used as the upper and lower limits of the 1-bit quantizer. Using these specific values will effectively mitigate the effect of the V^2 nonlinearity.

The other nonlinearity that must be overcome is the function $f(\theta)$ in equation (4). To circumvent this nonlinearity, a gain is introduced directly before the voltage is applied to the microphone. The additional feedback gain alters the signal levels of the biased pulse train to account for fluctuations in $f(\theta)$. The additional feedback gain required is,

$$G(\theta) = \sqrt{\frac{f(\theta^*)}{f(\theta)}}, \quad (8)$$

where $f(\theta^*)$ is a constant representing the $f(\theta)$ term at the biased operating point. By introducing this gain the effective transducer gain is,

$$f(\theta) \left(V \cdot \sqrt{\frac{f(\theta^*)}{f(\theta)}} \right)^2 = f(\theta^*) V^2. \quad (9)$$

This additional gain assumes that an accurate measurement of θ is available and the nonlinear function $f(\theta)$ is known. If an accurate measurement is available, then using the feedback linearization gain in equation (8) will result in a constant transducer gain. The combination of the feedback linearization gain and properly selected signal levels cancels the two nonlinearities.

3.2 Verification via nonlinear simulation with Simulink

Fig. 4 is the Simulink setup used to test the Sigma-Delta control loop proposed in this paper.

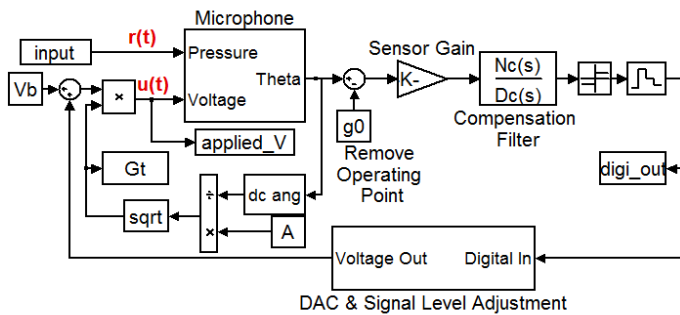


Fig. 4 Sigma-Delta Control Loop in Simulink

The input to the microphone is a short speech signal and the output is sensed and quantized with a sampling rate of 5 MHz providing a 1-bit oversampled pulse train. The digital signal is fed into a 1-bit DAC which outputs voltages of the appropriate signal levels. The voltage pulse train is added to a constant bias voltage and multiplied by an additional gain to maintain a symmetric electrostatic moment. The digital output is low pass filtered and decimated by a factor of 100 to reconstruct the input signal. A detailed design of a decimation process is described in Wu et al. (2004), but for this study a simple low pass filter and single stage decimator were used to reconstruct the signal. The digital low pass filter used is:

$$F(z) = \frac{10^{-5} \cdot (.5245z^2 + 2.07z + .5107)}{z^3 - 2.947z^2 + 2.895z - .9481}. \quad (10)$$

The low pass filter effectively averages the pulse train and extracts the signal contained in the density of the 1-bit output. Additionally, the digital low pass contains an integrator which will result in the tracking of the pressure as opposed to the pressure gradient. Fig. 5 compares the input signal versus the output of the open loop system and closed loop system. It can be clearly seen that the output of the open loop system does not track the system well because of the severe resonance at 1.6 kHz, while the closed loop system is able to successfully track the input speech signal when the resonance peak is damped. From the zoomed-in section of fig. 5, the resonance of the open loop response can be seen.

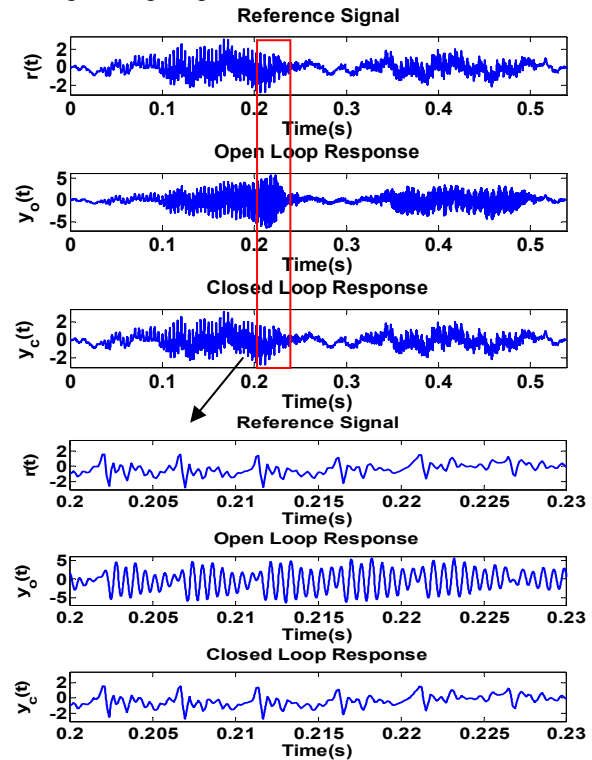


Fig. 5 Time domain response to a speech signal comparing original signal (top), open loop output (middle), and closed loop output (bottom). Zoomed-in open loop response shows resonance not present in the original signal and closed loop response. The control loop has removed the effect of the resonance.

The compensator described in this paper is a notch filter which cancels exactly the resonance peak of the microphone frequency response. Such a compensation scheme is inherently not robust. A small change in the natural frequency results in a significant distortion in the frequency response due to the mismatch between the notch from the analog filter and the peak from the microphone (See dashed line in Fig. 6). On the other hand, sigma-delta is insensitive to changes in the components in the forward path (Aziz et al. 1996 & Candy et al. 1992). Therefore the sigma-delta control loop should be tolerant to variations in the microphone's dynamics in spite of the non-robust compensator design. An additional simulation was conducted where the mass moment of inertia, I , and the torsional stiffness, k_t , were altered to simulate variability of the microphone fabrication. These two parameters determine the resonance frequency of the microphone. It has been observed that the parameters of fabricated microphone's vary

within 10% of specified values.. For this study the most extreme variations are considered.

3.3 Benefits of sigma-delta control to robust performance

Fig. 6 shows the magnitude plots comparing the simulation results of the sigma-delta response to the results of the linearized analog compensator systems. The mass-moment of inertia is decreased by 10% while the torsional stiffness is also increased by 10%, this results is a resonancel frequency shift from 1.6 kHz to 1.8 kHz (Fig. 6 top plot). Similarly, the mass-moment of inertia is increased by 10% and the torsional stiffness is decreased by 10% causing the natural frequency to shift to 1.45 kHz (Fig. 6 bottom plot). Despite the parameter variations, the sigma-delta control loop is able to track the input signal, whereas the linearized analog system is no longer able to damp the microphone's resonance. Although these simulations indicate enhanced robustness from the digital system, only two points in the possible parameter space are considered. Additional analysis must be conducted to insure that the robustness is valid over all possible parameter values.

An expected major benefit of using sigma-delta control is to circumvent the nonlinearity, and thus reduce signal distortion suffered when a large control signal is required. The control effort required for the closed loop tracking is shown in fig. 7. Contrary to the control effort required by the analog feedback controller in Miles et al., 2009b, the control effort of the sigma-delta loop is achievable given the constraints of the microphone. The voltage oscillates asymmetrically around the bias voltage of 3 V, while the additional correction gain remains around 1. Despite the correction gain's small range, it is a necessary element in order to prevent the reconstructed signal from drifting in a ramp fashion. Although a sigma-delta modulator is very tolerant to variations in analog devices in the forward path, the modulator is very sensitive to variations in the feedback path after the digital to analog converter (Aziz et al. 1996 & Candy et al. 1992). Additional study needs to be conducted to determine precisely how accurate the control voltage must be in order to provide a beneficial closed loop response.

4. CIRCUIT SIMULATION

A linear circuit is developed as a preliminary step in the implementation of a sigma-delta control system. The circuit contains a modified sigma-delta converter, where the loop is broken to include the linearized microphone dynamics and loop shaping filter. The nonlinearities from the capacitive actuator are assumed to be dealt with using the methods previously mentioned in section 3, and thus the nonlinearities are not included in the circuit simulation. Additionally, to prevent any issues arising from small signals in the circuit, the applied moments (due to sound and electrostatic actuation) are scaled up to be in the volt range. Although these simplifications are made, it does not affect the principle of operation of the control loop.

To confirm the functionality of the circuit, a random signal is injected and compared with the reconstructed output. The circuit simulation is performed with National Instrument's Multisim and a screen shot of the circuit is shown in Fig. 8.

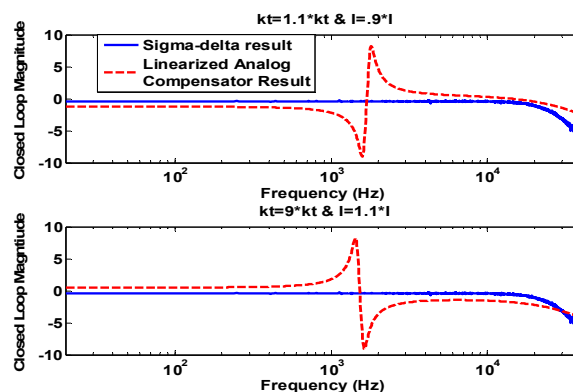


Fig.6 Magnitude plots of sigma-delta control loop vs closed loop linearized analog compensator. Top Plot - Microphone parameters are varied to shift the natural frequency from 1.6 kHz to 1.8 kHz. The strictly analog compensator result (dashed line) is compared with the result of the sigma-delta simulation (solid line) showing the insensitivity of sigma-delta. Bottom Plot - Microphone parameters varied to shift natural frequency from 1.6 kHz to 1.45 kHz.

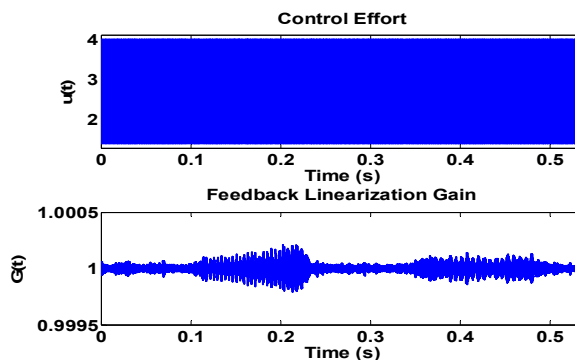


Fig.7 Control Effort & Feedback Linearization Gain. The control effort is a bipolar signal which oscillates between 4V and 1.414 V.

The circuit in Fig.8 is a simple implementation of a first order sigma-delta modulator obtained from Analog Device's application note on sigma-delta ADCs. A comparator and D flip-flop sampling at 5 MHz are used for the quantization process, and the digital signal is input to a 1-bit DAC which creates a NRZ analog signal. The analog signal is low pass filtered to provide the reconstructed output and is also used as a feedback signal.

Fig.9 shows the injected and the reconstructed time domain signals. It is clearly seen that the reconstructed signal is tracking the injected signal once the sigma-delta control loop enters its normal operation regime at the over-sampled frequency. The tracking confirms that the control loop is operating correctly in the circuit simulation environment. In addition to the tracking ability of the circuit, the robust performance shown in the Simulink simulation is also validated in the circuit implementation. The robustness of the circuit is tested in the same way as the Simulink Simulation. Additional work is currently being done to adapt the circuit model to include the nonlinear elements from the capacitive transducer.

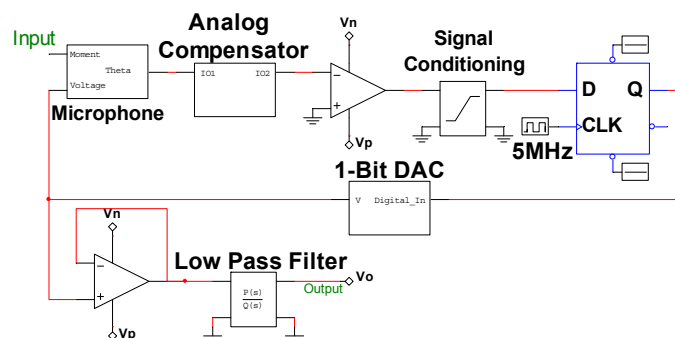


Fig.8 Closed loop sigma-delta control loop circuit with Multisim.

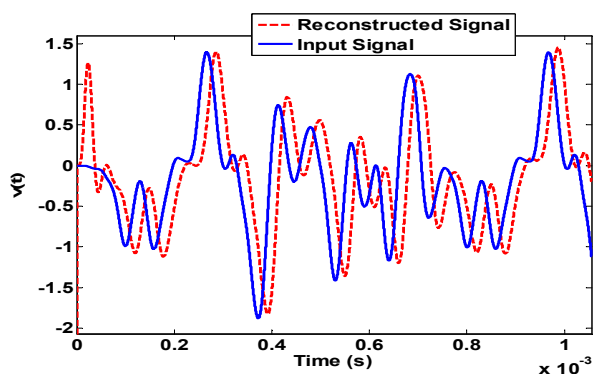


Fig.9 Time domain signals obtained from the sigma-delta control loop circuit. The reconstructed signal tracks the injected signal once the control loop enters its normal operation regime at the over-sampled frequency.

5. CONCLUSION

This paper presented the results of applying an active damping scheme to a biased and initially displaced directional microphone. Similar to Wu et al. (2004), a sigma-delta modulator was used to circumvent the nonlinearity due to the voltage. The device considered in this paper, however, operated under an asymmetrical condition due to the bias voltage and initial diaphragm angular displacement. Also taking into consideration in this paper was the effect of the rotation of the membrane on the electrostatic force. To overcome the nonlinearity of the asymmetric operation, the two signal levels of the bipolar feedback signal were adjusted to invert the nonlinearity. Feedback linearization was used to mitigate the fluctuations superimposed on the bipolar control signal due to the motion of the membrane. A simulation which includes the nonlinear elements of the capacitive transducer was developed in Simulink to validate the above measures and to analyze the robustness of sigma-delta control loop. The results of the simulation showed the elimination of resonance and thus improved tracking of the closed loop system. They also strongly supported the claim of robustness unique to the sigma-delta control loop. A preliminary circuit simulation was developed and tested to confirm proper functionality of the control loop. Additional work must be done to further confirm the robustness, develop a nonlinear circuit simulation, and insure the low noise is maintained in the closed loop system.

6. ACKNOWLEDGEMENT

This work was supported in part by the U.S. National Institute of Health under Grant 1R01DC009429-01.

REFERENCES

- Analog Devices, "Sigma-Delta ADCs and DACs", Application note AN-283.
- Aziz, Sorensen, and van der Spiegel, 1996, "An overview of sigma-delta converters", IEEE Signal Processing Magazine, pp.61-84, Jan.
- Bicen, B., Jolly, J., Jeelani, K., Garcia, C., Hall, N., Degertekin, F.L., Su, Q., Cui, W., Miles, R.N., 2009, "Integrated optical displacement detection and electrostatic actuation for directional optical microphones with micromachined biomimetic diaphragms", IEEE Sensors Journal, vol.9, pp.1933-1941.
- Candy, J. C., Temes, G.C., editors, 1992, Oversampling Delta-Sigma Data Converters: Theory, Design, and Simulation, IEEE Press,
- Cui, W., Bicen, B., Hall, N., Jones, S., Degertekin, F. L., and Miles, R. N. (2006). "Optical sensing in a directional MEMS microphone inspired by the ears of the parasitoid *Ormia ochracea*", in Proc. 19th IEEE Int. Conf. Micro Electro Mech. Syst., MEMS, 614{617 (Istanbul, Turkey).
- Kraft, M., 1997, Closed Loop Digital Accelerometer Employing Oversampling Conversion, Ph.D. Thesis, Coventry University
- Lemkin, M., and Boser, B.E., 1999, A three-axis micromachined accelerometer with a CMOS position-sense interface and digital offset-trim interface, IEEE Journal of Solid State Circuits, vol.34, pp.457-468
- Mason, A. C., Oshinsky, M. L., and Hoy, R. R., 2001, Hyperacute directional hearing in a microscale auditory system, Nature, vol. 410, pp.686-690.
- MathWorks, 1999, "Using Simulink"
- Miles, R. N., Su, Q., Cui, W., Shetye, M., Degertekin, F. L., Bicen, B., Garcia, C., Jones, S., and Hall, N., 2009a, "A low-noise directional microphone inspired by the ears of the parasitoid *Ormia ochracea*", J. Acoust. Soc. Am. 125, 2013-2026.
- Miles, R. N., Su, Quang T., Cui, W., Homentcovschi, D., 2009b, "Analysis and design of a MEMS directional microphone diaphragm with active Q control", ASA, 158th Meeting, Baltimore, MD
- Miles, R. N., Robert, D., and Hoy, R. R., 2005, "Mechanically coupled ears for directional hearing in the parasitoid fly *Ormia ochracea*," J. Acoust. Soc. Am. 98, 3059-3070.
- National Instruments, 2007, "Multisim User's Guide"
- Su, Q. T., Miles, R. N., Cui, W., Shetye, M., Wu, N. E., 2009, "Response of a MEMS directional microphone diaphragm with active Q control", ASA, 158th Meeting, Baltimore, MD.
- Wu, N. Eva , 2008, Feedback structure and asymmetric issues in digital control implementation of micromachined directional microphones, 9/5/2008 Progress Report to NIH
- Wu, Miles, Aydin, 2004, "A digital feedback damping scheme for a micromachined directional microphone", Proc. American Control Conference